Self Consistent Field Theory Study of Tetrablock Terpolymer Phase Behavior

A THESIS
SUBMITTED TO THE FACULTY OF THE GRADUATE SCHOOL
OF THE UNIVERSITY OF MINNESOTA
BY

Lynn M Wolf

IN PARTIAL FULFILLMENT OF THE REQUIREMENTS
FOR THE DEGREE OF
MASTER OF SCIENCE

Frank Bates, Adviser
Lorraine Francis, Adviser

August 2013

For my Mom

Acknowledgments

I never imagined so much would happen in my years in graduate school. I have never been so challenged or so rewarded in all of my life. My five years have been filled with professional development as well as a large amount of personal growth. I have had many positive influences and interactions from mentors and peers. Thank you to everyone for taking an active role and contributing so much to my life. It would take many pages to thank *everyone* indiviually so the following is a very abbreviated list.

My advisers Frank Bates and Lorraine Francis, have encouraged me throughout my hardships. After my accident, they both strongly supported my return to research and inspired me to work hard on completing my degree. Frank never lacked the time to guide me despite his assiduous schedule. He has helped me not only in my graduate career but also in my future plans. Lorraine has also given me great advice everything from research to my future plans. She supported me in many ways including supporting my return to research.

David Morse has helped in my understanding of Self Consistent Field Thoery. I have enjoyed the ability to take advantage of his open door policy when needing his expertise. He was always willing to help me gain a better understanding of the fundamentals of polymer thoery. His immense help is very much appreciated.

Eric Cochran gave me the opportunity to start my research career seven years ago. I much enjoyed the time I spent working for him and learning from his abundant knowledge. He not only taught me in class, in research but also in life. While working with Eric, I was given the chance to work with Ross Behling. Ross proved to me that life as a researcher can be fun and to never forget work ethic matters. While at Iowa State, I was also given the chance to work with Monica Lamm. She taught me how to ask the important questions and showed me the things in life that really matter.

Jeremy Riesberg has been a great friend since undergraduate work and I am not sure I would have kept my sanity without him. Katie Crawford provided me not only friendship but also encouragement in research and life over the seven years we have known each other. Billi Herman provided me with many encouraging words over some of the hardest months of my life. Megan Fuller, Jill Vollmuth and Roma Makell never stopped supporting my goal of returning to school. Many others have made my time

in graduate school rewarding in friendship and assistance in research including Karen Hamen, Tessi Panthani, Pravani Medapuram, Alex Mannion, Jeff Ting, Sangwoo Lee, Sangwon Kim, Carmelo Declet-Perez, Tim Gillard, Aaron Hedegaard, Brock Hedegaard, Joel Thomas, Scott King, Ben Swiniarski, Christina Braken-Thal and Kelly Best.

A special thanks to everyone at Quality Living Incorporated (QLI) for all their help, encouragement, reassurance and smiles they gave me in my recovery.

Contents

List of Tables

LIST OF TABLES

List of Figures

LIST OF FIGURES

LIST OF FIGURES

CHAPTER 1

Introduction

Polymerization techniques have progressed dramatically since Goodyear pioneered rubber vulcanization in the 1800's. Modern synthetic polymerization chemistry has allowed for a rapidly expanding portfolio of polymer architectures. A vast array of monomers can be used to create block and graft copolymers that take on many architectures. Linking the morphological features of a copolymer with it's physical properties provides an ever growing challenge to polymer scientists and engineers. This introduction will focus on the advancement of knowledge in tetrablock terpolymer structures in the last five years.

Self-assembly of block copolymers into periodically ordered microstructures is an advantageous way to create materials with strict control over length scale and mor-

phology.[7] Block copolymers microphase separate to minimize free energy by reducing unfavorable monomer contacts while maintaining uniform density and minimizing the entropy reduction associated with chain stretching. The simplest example is linear diblock copolymers, AB diblocks, which generate six stable phases, four of which are produced with almost any pair of polymers. At a strong or intermediate segregation strength (χ_{AB}N $\gg$10, where χ_{AB} is the Flory-Huggins segment-segment interaction parameter and N is the degree of polymerization), morphology is determined solely by minority block volume fraction(f). High asymmetry ($f \sim$ 0.1-0.15) leads to spherical domains of the minority component with BCC order in a matrix of the majority block. Decrease in the asymmetry ($f \sim$ 0.15-0.3) leads to hexagonally packed cylinders of the minority domain. Alternating lamellae of A-rich and B-rich domains are stable when the volume fractions of both components are comparable ($f \sim$ 0.35-0.5). These "classical" phases are accompanied by a bicontinuous double gyroid, which occurs over a narrow region of composition space between lamellae and cylinders ($f \sim$ 0.3-0.35). Block conformational asymmetry[8] and polydispersity[9] can shift these morphological boundaries but the overall topology of the AB diblock phase portrait remains unperturbed. Recently the "classical" phases have been joined by two more complex phases.

Bicontinuous structures that were initially identified as double-diamond were subsequently shown to be gyroid structures.[10,11] Both theory and synthesized polymers played critical roles in unraveling the molecular factors responsible for the formation of the gyroid phase. Several years ago, self-consistent field theory (SCFT) anticipated a fifth stable phase in diblock copolymers, an orthorhombic network struc-

tured, dubbed O^{70}, with $Fddd$ symmetry.[4] Soon after publication of this theoretical work, experiments revealed the existence of O^{70} for poly(styrene-**b**-isoprene).[12] Recently the σ-phase has been documented in a low molecular weight sphere forming poly(isoprene-**b**-lactide) diblock copolymer melt using synchrotron SAXS and TEM.[6] Lee et. al point out that this sixth phase has not been accounted for theoretically.[6] The predicted phase diagram to date complete with the O^{70} but lacking the σ-phase is shown in Figure 1.1.

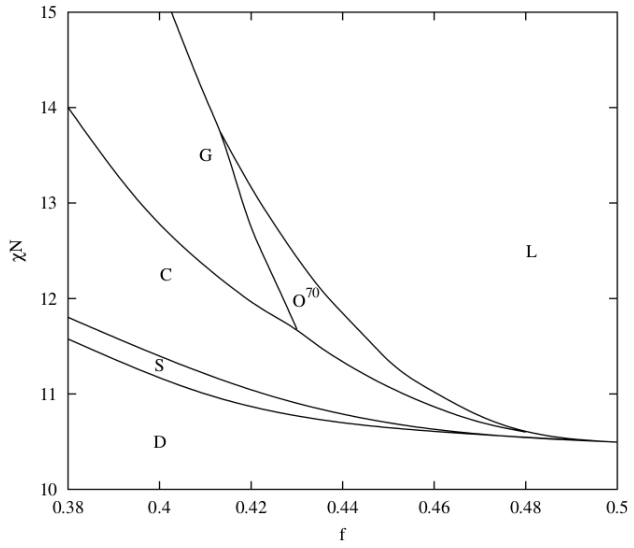

Figure 1.1: Theoretical phase diagram for diblock copolymers to date. This includes the disordered phase (D), BCC spheres (S), hexagonally packed cylinders (C), gyroid (G), the O^{70} and lamelle (L). The σ phase has not yet been accounted for using theory. The O^{70} phase is only seen under a small parameter space that was earlier considered to be gyroid. Figure taken from Tyler and Morse.[4]

The complexity of phase formation is extensively expanded by the addition of more blocks. For example, addition of a third block triples the number of possible interfaces (A/B, A/C, and B/C) complicating the free energy balance that determines the self-assembly behavior of the triblock terpolymer. Linear triblock terpolymers have more than 30 known ordered morphologies with more likely to be discovered.[13–20]

There is an attractive design flexibility in using three chemically distinct blocks (e.g. glassy, rubbery, semi-crystalline domains arranged in tailored microstructures). Distinct blocks also give a vast array of structural choices. SCFT provides crucial guidance in relating the block sequence and interaction parameter (χ_{AB}, χ_{AC} and χ_{BC}) to the morphology of the terpolymer as evidenced by successfully modeling entire ABC phase portraits.[21–23] The thermodynamic driving force for block segregation is governed by the segment-segment interaction parameters, χ_{AB}, χ_{AC} and χ_{BC}, the composition, and the overall molecular weight. When $\chi_{BC} > \chi_{AB} \approx \chi_{AC}$, contact between the B and C blocks is unfavorable leading to domain structures that avoid B/C interfaces. This system is also known as a 'frustrated' system because the two blocks with the greatest interaction are covalently bonded to each other, forcing an undesirable interaction. Analogous to AB diblocks, core-shell gyroid, cylinders and spheres have been reported in ABC triblock terpolymers.[18–20] For example, the cubic gyroid phase has been reported in at least three forms: two-monomer gyroid (G), three-monomer core-shell gyroid (Q^{230}), and three-monomer alternating gyroid (Q^{214}).[15,19] In all cases these structures are formed by a single set of symmetric three-fold junctions fitted with equal length tubular connectors.[15]

Another class of network phases, characterized by orthorhombic(O) symmetry,

have also been reported.[15,24] The structural elements of these networks are similar to the cubic networks however the overall symmetry is lower and the junctions are not three-fold symmetric. An equilibrium network that has been identified is the O^{70} ($Fddd$ space group symmetry)[13], while a metastable O^{52} ($Pnna$) was achieved by applying strong shear.[24] Orthorhombic lattices consist of three different unit cell lengths making these networks somewhat flexible. This may explain the wide composition range over which the O^{70} have been found in linear ABC triblock terpolymers.

It is believed that BABC tetrablock terpolymer architcture affords the polymer scientist and engineer a rich set of new design options. For example, ABA triblocks make excellent thermoplastic elastomers and tough plastics. Addition of a fourth chemically distinct block can direct this mechanically robust unit into otherwise inaccessible morphologies depending on relative magnitude of χ_{AB}, χ_{AC} and χ_{BC}. This concept, along with others, has motivated the exploration of self-assembly behavior of BABC tetrablock terpolymers.

A formula has been developed (ménages en blocs) that determines the number of possible linear polymer structures that can be formed given the number of blocks as well as the number of monomers used.[25] For tetrablock polymers with three different species, there are 9 possibilities.[25] Tetrablock terpolymers are refered to as BABC terpolymers in this thesis. The choice of length of the C block, N_C, relative to the length of B blocks, N_B, $N_{B'}$, and length of the A block N_A, offers control over the domain curvature (e.g., spherical or cylindrical domains), while the magnitudes of χ_{AB}, χ_{AC}, χ_{BC} and $\xi = N_{B'}/N_B$ and the overall block polymer size, N = ΣN_i, dictate the morphology of the surrounding matrix.

Polymers consisting of multiple blocks of chemically distinct units are characterized in multiple ways to ensure accurate structure assignment. Gel permeation chromatography (GPC) and ^{1}H NMR are used to determine molecular weight. Volume fraction is found using previously determined polymer densities.[26] This information is supplemented with small angle X-ray scattering(SAXS) and transmission electron microscopy(TEM) to determine structural elements. The peak data seen in SAXS is compared to images obtained through TEM to accurately determine structure.

Unanticipated network structures have been found in tetrablocks. In the effort finding more network structures, asymmetric BABC terpolymers were persued. Bluemle et al. delved into this using poly(cyclohexylethylene-**b**-ethylene-**b**-cyclohexylethylene-**b**-dimethylsiloxane) (CECD) as the tetrablock copolymer and studied the phase formations of this polymer with varying lengths of the D block.[5] The asymmetric aspect can be seen in the two separate blocks of C. This polymer was synthesized using previously published polymerization techniques involving sequential anionic polymerization of styrene, butadiene, styrene and hexamethylcyclotrisiloxane.[27] The tetrablock terpolymer was then hydrogenated over a silica-supported platinum/rhenium catalyst. This polymer is enticing because it combines glassy ($T_{g,C} \cong 135$ °C), semi- crystalline ($T_{m,E} \cong 100$ °C), and rubbery ($T_{g,D} \cong 130$ °C) elements in a single compound.[5]

At low volume fraction of polydimethylsiloxane (PDMS), the tetrablock terpolymer takes the form of hexagonally packed cylinders. Upon increasing the length of the PDMS domain, an ordered O^{52} phase is observed. This phase is orthorhombic in nature and has $Pnna$ space group symmetry. A ball and stick model of this space group can be seen in Figure 1.2. Further increase in the amount of PDMS led to the

formation of core-shell cylinders. It was rationalized that the tetrablock architcture produced the three-fold junctions needed to make the O^{52} morphology. An illustration of the structures observed based on the volume fraction of PDMS can be seen in Figure 1.3.

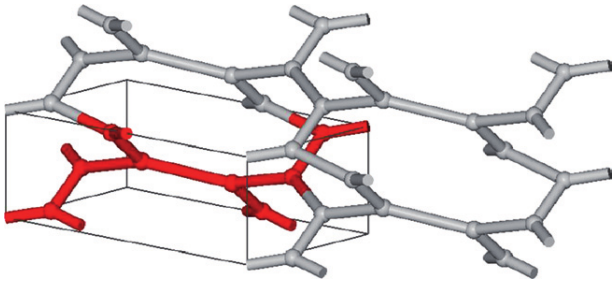

Figure 1.2: Ball and stick representation of 4 unit cells of the *Pnna* network phase. The wire frame denotes one unit cell. Figure reproduced from Bluemle et al.[5]

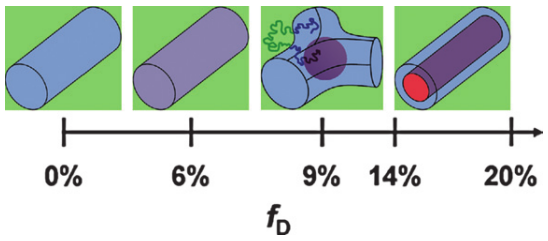

Figure 1.3: Local structure of CECD based phases with increasing volume fraction of PDMS. The O^{52} network phase is seen at f_D=0.09. Figure reproduced from Bluemle et al.[5]

CEC (0% PDMS) consists of cylinders of C embedded in an E matrix. PDMS mixes with the cylindrical C domains at compositions up to 6% PDMS. A microphase separation of the PDMS block is induced by further increasing the amount of PDMS to about 9% D. The formation of spheres of D is expected due to the small overall volume fraction of D . Confining a sphere within a cylinder is likely to cause some packing problems. It is important to note the interaction parameters favors D/C and

E/C contacts and not E/D interfaces. Transformation of the cylinders into three-fold junctions would allow for the D domains to be isolated within the C. The terminal C block has room to wander away from the vicinity of D domains and enter the C struts closer to the midpoint between the three-fold junctions as seen in Figure 1.3. Increasing the length of the D block reduces the interfacial curvature leading to the formation of D cylinders. Surrounding the cylinder of D with a shell of C satisfies the interaction parameter constraints. These cylinders are hexagonally packed in a continuous matrix of E. There has been no subsequent theory work to show if the observed O^{52} structure is a thermodynamically stable equilibrium phase or a metastable phase.

The majority of tetrablock terpolymers studies have investigated the bulk morphological behavior of poly(styrene-**b**-isoprene-**b**-styrene-**b**-ethylene oxide) SISO terpolymers. These polymers were synthesized following protocol explained in previous work.[27,28] This method ensures that the only variation in this series of polymers is the length of the O block.

Bluemle et al. completed the first work done probing the structures formed by SISO tetrablock terpolymers.[3] This early work dealt with polymers where $f_S = f_I$ and f_O between 0 and 30% (the S is divided equally between the two S blocks). The parent block used to synthesize subsequent tetrablocks was SIS consisting of 25.5% S, 49% I, 25.5% S. This triblock was disordered at 80 °C. A small addition (4% O) did not show any change from this disordered state. Liquid-like packing of spheres was observed for $0.07 < f_O < 0.09$. TEM images of this formation confirmed the results that were found in the SAXS data for this sample. Further increasing the O volume

fraction to 12% resulted in the formation of hexagonally packed cylinders. This result was consistently seen up to the highest volume fraction(30% O). The increase in O volume fraction had a minimal effect on morphological length scale of the cylinder phase. The microstructures observed with these sample are reproduced in Figure 1.4.

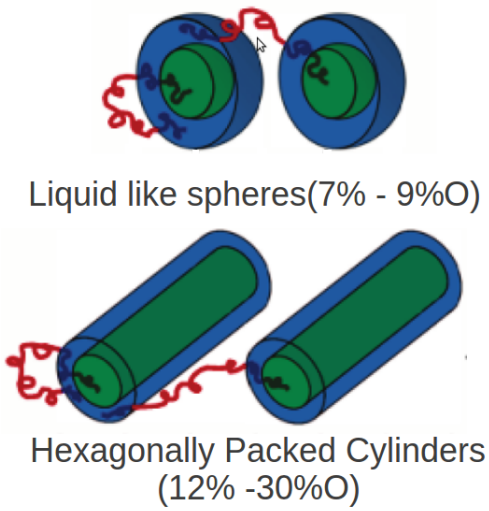

Figure 1.4: Local structure of SISO phases with an increase in O volume fraction. At lower volume fractions (7% - 9%D) core shell spheres are seen. At higher volume fractions (12% - 30%D), core shell cylinders are observed. Figure partially reproduced from Figure 3 of Bluemle et al.[3]

The core-shell morphologies observed with SISO tetrablocks differ significantly from the morpholoies seen in ISO triblock copolymers of similar compositions. An orthorhombic structure (O^{70}) with $Fddd$ symmetry was stable over a wide range of O volume fractions ($0.13 \leq f_O \leq 0.24$) along the $f_I = f_S$ isopleth in SISO.[15] It was concluded that changing the molecular architecture from ISO to SISO drives a preference from the hyperbolic interfaces in network phases, like O^{70}, to zero and positive Gauss curvature surfaces present in cylinders and spheres.[3]

With the polymers synthesized by Bluemle, it was discovered that core(O)-shell(S) cylinder microstructure was favored even at $f_O = 0.30$.[3] Previously, an inverted cylindrical phase (where the minority component forms a continuous domain) had been seen in the past with SIO,[27] poly(isoprene-**b**-styrene-**b**-dimethylsiloxane),[29] and certain diblock/triblock blends.[30] The inverted phases occured when the interaction parameters were asymmetric ($\chi_{BC} > \chi_{AB} \cong \chi_{AC}$). This is not the case for ISO where $\chi_{AC} > \chi_{AB} \cong \chi_{BC}$. These results suggest that BABC tetrablocks can produce very different ordered structures than found in ABC triblocks of the same composition.

Zhang et al. investigated sphere forming SISO tetrablock terpolymers that are arranged on a hexagonal lattice.[2] The spheres appear to have $P6/mmm$ symmetry. Simple hexagonal packing is extremely rare, most elements pack into either face centered cubic(FCC), body centered cubic(BCC) or hexagonally close packed(HCP). This symmetry has not been observed in single component crystals but has been reported in intermetallic compounds.[31] BCC packing is commonly seen in a single component asymmetric block copolymer[32] as anticipated by Leibler.[33]

The arrangement of SISO inverts the block placement with the interaction param-

eters because $\chi_{SI} \leq \chi_{SO} \ll \chi_{IO}$. This discourages contact between the I/O domains leading to spheres of O to form in a shell of S in a matrix of I and S.[2] Previously tested synthesis techniques[27] were used to create blocks of various O length with a parent SIS triblock (40% S).[2]

The phase portrait of the SISO tetrablock terpolymers system used by Zhang et al. can be found in Figure 1.5. This figure does not take into account the role of χN, which would form a fourth axis. Because of the use of one parent SIS triblock, the materials synthesized fall along the isopleth of constant f_S and f_I with a varying f_O. Because the blocks of S are symmetric, this work focused on tetrablocks where N_S=$N_{S'}$.

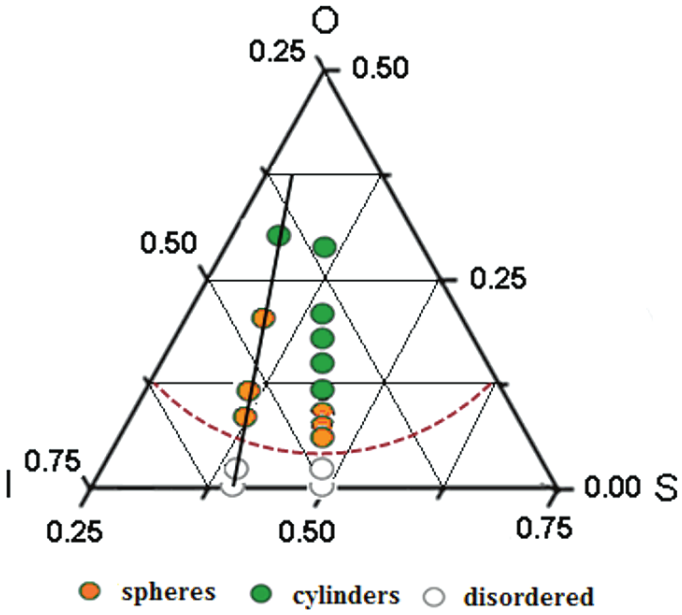

Figure 1.5: Phase portrait of poly(styrene-**b**-isoprene-**b**-styrene-**b**-ethylene oxide) (SISO) near the order-disorder transition depicted as the dashed curve. Filled and open circles indicate ordered and disordered states, respectively, within the experimental temperature range 100 $\leq$ T $\leq$ 250 °C . The isopleth with 50 vol % S and 50 vol % I was published elsewhere.[3] Figure reproduced from Figure 2 of Zhang et al.[2]

Figure 1.5 contains two isopleths, one with f_S = 1-f_I = 1/2 which was shown in earlier publications[3] as well as the isopleth looked at by Zhang where f_S=0.39.[2] This was done to bridge the order-disorder transition with increasing O as previously reported by Epps et al.[15] Based on SAXS patterns, TEM images and rheological measurements it was concluded that hexagonally packed spheres were present with samples that contained 9-19% O and cylinders were present at 32% O.

SCFT calculations have shown the formation of BCC symmetry given the sphere morphology[33] but do not account for this experimental simple hexagonal spherical packing ($P6/mmm$ symmetry). Density profiles from SCFT (Figure 1.8 indicate that the actual mophology observed is a mix of illustrations (2) and (3) depicted in Figure 1.6. The density profile of the higher O containing terpolymer can be seen in Figure 1.8. This specimen has $P6/mm$ space group symmetry.

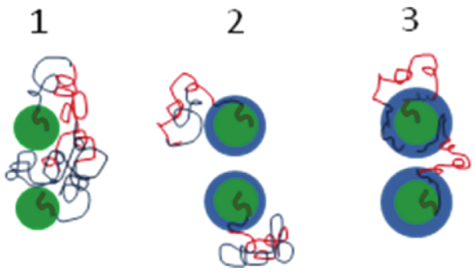

Figure 1.6: Discrete states of microphase separation for sphere forming SISO tetrablock terpolymers. (1) Segregated of O blocks from mixed inner and outer S and I blocks. (2) Segregated core of O surrounded by a shell of inner S blocks embedded in a matrix of mixed I and outer S blocks. (3) Core of O surrounded by a shell of segregated inner and outer S blocks enbedded in a matrix of I. Figure reproduced from Figure 8 of Zhang et al.[2]

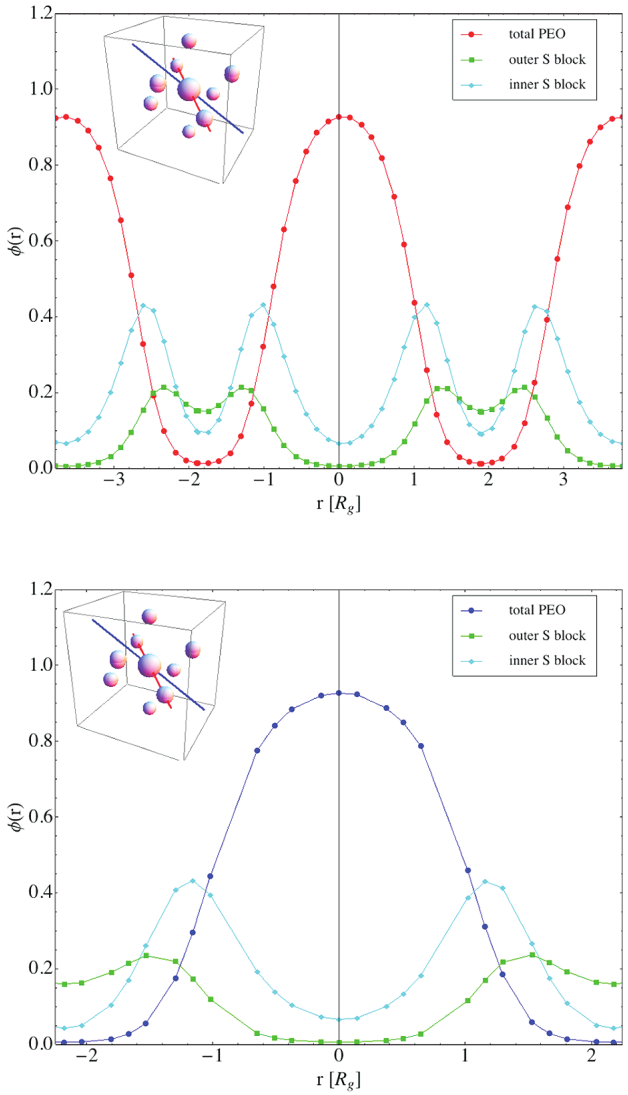

Figure 1.7: SCFT density profiles of O, terminal S and interior S' against position variable, r for one synthesized tetrablock. The top panel contains the profile along the [111] unit cell direction denoted by the red line. The bottom panel contains the [100] unit cell direction as denoted by the blue line. These results indicate that the SISO tetrablock terpolymers segregate with a distribuion of blocks that is a hybrid of models 2 and 3 in Figure 1.6. Figure reproduced from Figure 9 of Zhang et al.[2]

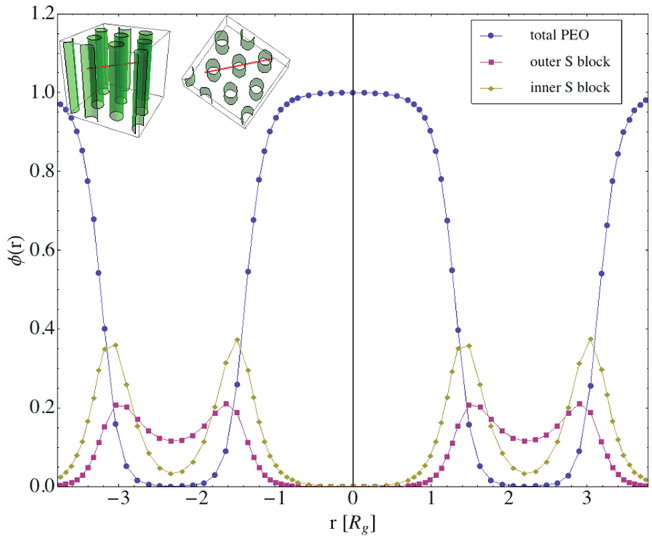

Figure 1.8: SCFT density profiles of O, terminal S and interior S' against position variable, r for one synthesized tetrablock. This shows the hexagonal $P6/mm$ symmetry observed for the f_O=0.32 polymer. The density profiles were calculated along the [100] unit cell direction as shown in the inset. Figure reproduced from Figure 10 of Zhang et al.[2]

This work has demonstrated the tetrablock terpolymer molecular architcture(SISO) introduces new levels of morphological control unavailable to the more convenient triblock copolymer(ISO). Unfavorable segment-segment interactions between I and O blocks drive the formation of spherical microdomains for f_O = 0.09, 0.12, 0.19 while at f_O = 0.32, the specimen contains a cylindrical morphology. It was concluded that the $P6/mmm$ space group symmetry for specimens containing f_S/f_I = 2/3 of poly(isoprene) and poly(styrene) block fractions (equal between the two S blocks) and between 9 and 32% poly(ethylene oxide).

An intriguing and new non-network structure that has been recently explored in tetrablock terpolymers as well as in diblock copolymers is the σ-phase by Lee et al.[6] This cubic $P4_2/mnm$ phase was first proposed for metallic alloys more than 50

years ago by Frank and Kasper. Powder SAXS patterns obtained for SISO tetrablock terpolymers and IL diblock copolymers confirm the assignment of the σ-phase. The unit cell of the Frank-Kasper σ-phase consists of 30 spherical particles in a tetragonal lattice[6] as seen in Figure 1.9.

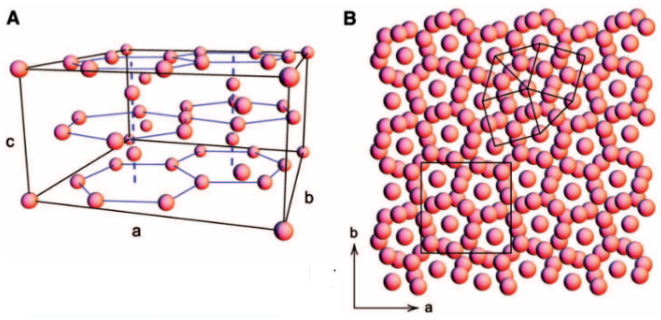

Figure 1.9: (A) Unit cell for σ-phase ($P4_2/mnm$ symmetry). Columns of spheres (dashed blue lines) surrounded by rings of hexagonally coordinated spheres (solid blue lines) produce a distinctive pattern along the c-axis(B). This is consistent with the TEM image seen for this sample. Figure reproduced from Lee et al.[6]

The σ-phase is an approximant crystal structure to certain dodecagonal quasicrystals and an example of both σ-phase and quasicrystal formation has been reproted in a single-dendrimer compound.[34,35] Using a similar SISO tetrablock where the σ phase was identified, a dodecagonal quasicrystalline formation was also observed. The intriguing state of dodecagonal quasicrystalline(QC) morphology was studied in work by Zhang and Bates.[36] It was found that this state occurs at a temperature between that associated with the σ-phase($P4_2/mmm$) and a phase with simple hexagonal order(HEX), $T_{HEX} < T_{QC} < T_\sigma < T_{ODT}$ where T_{ODT} is the order-disorder transition temperature. TEM work was done to show that this structure has a 12-fold rotational symmetry but is devoid of long range translational order along with locally coordi-

nated structures consistent with dodecagonal quasicrystalline approximations.[36]

In the work done by Lee et al., the σ-phase was seen with f_S=0.46, f_I=0.46 and f_O=0.08 with the S domain equally split between both domains.[6] The QC morpholoy was seen when f_S=0.35, f_I=0.56 and f_O=0.9.[36] The other interesting morphology of simple hexagonal ordering ($P6/mmm$) symmetry was seen with f_S=0.35, f_I=0.56 and f_O=0.9.[2] It was shown through scattering patterns obtained at varying temperatures that the QC phase was seen at 210°C[36] and the simple hexagonal ordering was seen when the sample was annealed for 1 day at 120 °C.[2] The QC phase started showing an increased number of scattering peaks between 160 °C and 190 °C. This led to further study using TEM images of samples annealed at various temperatures. This work showed that the QC phase formed at 175 °C.

SAXS experiments have revealed the sequence of the phases QC $\rightarrow P4_2/mnm \rightarrow$ isotropic in dendrimers[34] which has been attributed to molecular packing frustration.[37] This effect is well established in single component block copolymer melts, where compressing and stretching blocks away from preferred random-walk configurations is required in order to place domains (e.g spheres) on an ordered lattice at uniform polymer density.[38] In the mean-field limit, diblock copolymer spheres order on a BCC lattice;[32,33] however, recent work has shown that low molecular weight diblocks can form the σ-phase, presumably reflecting modified interdomain interactions due to Gaussian corona block chain statistics.[6]

There is good reason to believe that BAB′C type tetrablock terpolymers are attractive candidates for exploring new states of order in soft materials.[25] Inverted phases[3], O^{70} phase[3], O^{52} phase[5], spheres with $P6/mnm$ and $P6/mm$ symmetry[2],

the σ-phase[6], as well as a dodecagonal quasicrystalline state[36] have all been seen with a BABC tetrablock terpolymer. There is great potential for achieving a vast number of structures to be used in multiple applications.

This thesis reports the study of tetrablock terpolymer self assembly via Self Consistent Field Theory on two polymer systems. Chapter 3 will investigate the system of poly(styrene-**b**-isoprene-**b**-styrene-**b**-ethylene oxide) (SISO) that was studied by Bluemle and Zhang.[2,3] SCFT studies will be compared to the experimental results given by Bluemle and Zhang to better understand self assembly as well as the role that interaction parameters play.

CHAPTER 2

Self Consistent Field Theory Implementation

The statistical mechanics of polymer melts is a many-body interacting problem. Block copolymer melts separate into spatially inhomogeneous fluids that are ordered on the length scale of a polymer coil. The interactions between polymer chains make the statistical mechanics impossible to solve without approximations. Self Consistent Field Theory (SCFT) provides a means for calculating the free energy of an ordered polymer melt. SCFT is a mean field theory in which all interactions between polymers are approximated by interactions of each polymer with a set of chemical potential fields. Adding an unknown chemical potential field reduces the intractable many-chain problem to the tractable problem of an ideal gas of polymer chains.

A self-consistent field (SCF) approximation for polymers was first used to study

the size of a homopolymer with excluded volume interactions in solutions.[39] Edwards suggested that the distribution of polymer configurations may be approximated by that of a random walk in a potential field that is determined posteriori from the monomer concentration. SCFT was later adapted by Hefland and coworkers to describe inhomogeneous structures in dense multi-component polymer liquids,[40–42] such as interfaces between immiscible polymer liquids[40–42] and to block copolymer melts.[42–45] The interfacial tension was derived as a function of the Flory-Huggins interaction parameter. The result was later extended to the case of non-symmetric interfaces. The fundamental issues relating to their treatment to the Gaussian random walk were addressed. Subsequently the theory was developed to study the microdomain structure in a meso-phase seperated block copolymer melt. Then the Narrow Interface Approximation (NIA)[45] was introduced to study block copolymer melts in the Strong Segregation Limit (SSL). The stability of classical L (Lamellae), H (Hexagonal), and S (Sphere) phases found in diblock copolymer melts were also analyzed.[46,47]

2.1 SCFT Formalism

The SCFT equations were solved numerically first using spectral expansions developed by Schick and Matsen.[48] Their calculation produces the phase diagram for diblock copolymers in the full composition window covering the range of χN values from 0 to 120. The numeric SCFT is by far the most effective method for analyzing the phase behavior of block copolymer melts, the basic contents of which will be introduced in the next section.

The standard theoretical model to understand block copolymer phase behavior has become SCFT so only a brief summary is given here. The theory provides a statistical description of the spatial distribution of all interacting chains. Chain configurations are counted by a random walk model and monomer-monomer interactions are replaced by interactions between monomers and self-consistent built molecular fields. Both of these are valid approximations for long chains. The problem is to estimate the statistical weights of the Gaussian chains in external fields. Imagine a chain growing process for which each local step is biased by the external fields can be converted to a solution to the modified diffusion equations.

2.2 Modified Diffusion Equations

Consider an incompressible melt of a linear monodisperse multiblock copolymer, in which all chains have N monomers, each of which occupies the same volume, v. Let s denote the distance along the chain, defined such that $0 < s < N$. Let $\mathbf{r}$ represent that position in a system of a total volume V. Let $\phi_\alpha(\mathbf{r})$ represent the average volume fraction of monomers of type α at position $\mathbf{r}$, defined as the product of the average number such of monomers per unit volume times the monomer volume v. The singly constrained partition functions $q(\mathbf{r},\mathrm{s})$ and $q^\dagger(\mathbf{r},\mathrm{s})$ are proportional to the statistical weights of the random walks committed by the segments to the left and right sides of the s segment positioned at $\mathbf{r}$. They satisfy:

$$\frac{\partial q}{\partial s}(\mathbf{r},s) = \left[\frac{1}{6}b(s)^2\nabla^2 - \omega(\mathbf{r},s)\right] q(\mathbf{r},s) \tag{2.2.1}$$

$$-\frac{\partial q^\dagger}{\partial s}(\mathbf{r},s) = \left[\frac{1}{6}b(s)^2\nabla^2 - \omega(\mathbf{r},s)\right] q^\dagger(\mathbf{r},s) \tag{2.2.2}$$

subject to boundary conditions

$$q(\mathbf{r},0) = q^\dagger(\mathbf{r},1) = 1 \tag{2.2.3}$$

Here s has been normalized by N. $b(s)$ is the statistical segment lengths constants within a block. The exchange chemical potential fields $\omega_\alpha(\mathbf{r})$ are specific to monomers, so can be denoted $\omega_\alpha(\mathbf{r})$ as the s segment is of type α, α being monomer type index. The chemical potential field on a per monomer basis with units of kT is

$$\omega_\alpha(\mathbf{r}) = \sum_{\beta\neq\alpha} \chi_{\alpha\beta}\phi_\beta(\mathbf{r}) + \xi(\mathbf{r}) \tag{2.2.4}$$

where χ is the Flory Huggins interaction parameter for binary interation between α and β monomers for which $\chi_{\alpha\beta}$=$\chi_{\beta\alpha}$. By convention,

$\chi_{\alpha\alpha} = \chi_{\beta\beta} = 0$.

Here $\xi(\mathbf{r})$ is a Langrangian pressure field adjusted to produce a constant density:

$$\sum_\alpha \phi_\alpha(\mathbf{r}) = 1 \tag{2.2.5}$$

Note that $\phi_\alpha(\mathbf{r})$ has been normalized by the overall density. The density fields are calculated from solutions to Equation 2.2.3:

$$\phi_\alpha(\mathbf{r}) = \frac{1}{Q}\int_\alpha ds\, q(\mathbf{r},s)\, q^\dagger(\mathbf{r},s) \tag{2.2.6}$$

where $\int_\alpha$ means the summation over all s segments of the type α. The normalization constant is the partition function:

$$Q \equiv \frac{1}{V}\int d\mathbf{r}\, q(\mathbf{r},s)\, q^\dagger(\mathbf{r},s) = \frac{1}{V}\int d\mathbf{r}\, q(\mathbf{r},1) \tag{2.2.7}$$

The last identity used the fact that the definition is independant of s.

After the self-consistent solution is found, the free energy of a single chain is calculated by:

$$f = -\ln(Q\mathbf{e}) + \frac{N}{2V}\sum_{\alpha,\beta}\chi_{\alpha\beta}\int d\mathbf{r}\, \phi_\alpha(\mathbf{r})\, \phi_\beta(\mathbf{r}) - \frac{1}{V}\sum_\alpha \int d\mathbf{r}\, \omega_\alpha(\mathbf{r})\, \phi_\alpha(\mathbf{r}) \tag{2.2.8}$$

SCFT is used to solve Eq 2.2.3, 2.2.4 and 2.2.5 inside a unit cell self consistently with each solution being periodic.

2.3 Pseudo-Spectral Method

The homogeneous solution cooresponds to the Flory-Huggins theory for a disordered melt. We aim to resolve the others which can be represented by coarse grained pictures of ordered morphologies. Comparing the free energies allows for the determination of the thermodynamically stable phase. The algorithms for solving the modified diffusion equations and iterating $\phi(\mathbf{r})$ fields are done using the pseudo-spectral method.

A spectral solution was developed by Matsen and Schick to solve the Modified Diffusion Equation (MDE).[48] The solution used symmetry adapted basis functions. From this method, the three dimensional gyroid and BCC sphere phase were successfully simulated. The governing MDE is reduced to the form of

$$\frac{\partial q}{\partial s}(\mathbf{r}, s) = -Hq(\mathbf{r}, s) \tag{2.3.1}$$

where H cooresponds to the operator

$$H \equiv \left[-\frac{1}{6}b(s)^2\nabla^2 - \omega(\mathbf{r}, s)\right] \tag{2.3.2}$$

The solution for the MDE in their case is obtained by propagating from the initial condition of $q(r, 0) = 1$ for a given set of chemical potentials for each monomer $\omega(r)$ through the relation

$$q^{(1)}(\mathbf{r}, s + ds) = \exp\left[ds\left(\frac{Nb(s)^2\nabla^2}{6} - N\omega(\mathbf{r}, s)/2\right)\right] q(\mathbf{r}, s) \tag{2.3.3}$$

The time taken to solve the MDE is found to scale as M^3, where M is the number of symmetry basis functions used to resolve the space group of the periodic phase. In comparison, the pseudo-spectral formulation developed by Rasmussen and Kalosakas[49] scales as $MN_{grid}\log(N_{grid})$ where M is the number of grid points involved in the discretation of the contour variable s and N_{grid} is the number of grid points for spatial discretation, The pseudo-spectral formalism has been implemented by Qin and Morse and a more-detailed description of this method can be found in Qin's thesis.[50] Here we summerize the pseudo-spectral formalism used to simulate

periodic phases.

The propagator in this case is complicated to evaluate as $\omega(\mathbf{r}, s)$ is diagonal in real space and ∇^2 is diagonal in reciprocal space. In the case of pseudo-spectral formalism the propagator exp(-H) is given by the approximation

$$\begin{aligned} &q(\mathbf{r}, s+ds) \backsimeq \\ &\exp\left(-\tfrac{\omega(\mathbf{r},s)}{2}ds\right)\exp\left(\tfrac{b^2\nabla^2}{6}ds\right)\exp\left(\tfrac{-\omega(\mathbf{r},s)}{2}ds\right)q(\mathbf{r},s)+\mathcal{O}(ds^3) \end{aligned} \tag{2.3.4}$$

In the pseudo-spectral algorithm the $\omega(\mathbf{r}, s)$ operating on $q(\mathbf{r}, s)$ is calculated in real space and $\nabla^2 q(\mathbf{r}, s)$ is calculated in Fourier space with the help of the fast Fourier transforms.

$$q^{(1)}(\mathbf{r}, s+ds) = \exp(-ds\,\omega(\mathbf{r}, s)/2)q(\mathbf{r}, s) \tag{2.3.5}$$

$$q^{(1)}(\mathbf{r}, s+ds) = \mathcal{FFT}\left[q^{(1)}(\mathbf{r}, s+ds)\right] \tag{2.3.6}$$

$$q^{(2)}(\mathbf{r}, s+ds) = \exp(-ds\,b(s)^2\left|G_k\right|^2/6)(\mathbf{k}, s+ds) \tag{2.3.7}$$

$$q^{(2)}(\mathbf{r}, s+ds) = \mathcal{FFT}^{-1}\left[q^{(2)}(\mathbf{r}, s+ds)\right] \tag{2.3.8}$$

$$q(\mathbf{r}, s+ds) = \exp(ds\,\omega(\mathbf{r}, s)/2)q^{(2)}(\mathbf{r}, s+ds) \tag{2.3.9}$$

Propagation of the intial condition $r(\mathbf{r}, 0) = 1$ will yield an approximate solution

to Equation 2.2.3 for any periodic input $\omega(\mathbf{r}, s)$. Space group symmetry is not needed for this. An analogous scheme can be designed for $q^{\dagger}(\mathbf{r}, s)$.

A set of symmetry adapted basis functions which capture the symmetry of the particular space group are generated in order to calculate the residual. The generation of symmetry adapted basis functions was implemented for the spectral formalism by Tyler and Morse,[51] and for the pseudo-spectral formalism was extended by Qin and Morse.[50] One needs to specify a reference state for a canonical ensemble as mentioned previously for the real space formulation of SCFT. In the case of PSCF, the Lagrange field of the homogenous componenet of PSCF is set to zero $\xi(\mathbf{G} = 0) = 0$ in order to take care of homogenous shifts in $\xi(\mathbf{r})$ yeilding the same solution. For the grand canonical ensemble the Lagrange field $\xi(\mathbf{r})$ is uniquely determined for each grid point or basis functions.

2.4 Iterations

Once the MDE has been solved for the periodic phases the solution has to be iterated to get the required tolerance under the constraints mentioned earlier for the real space formulation of SCFT. For the case of PSCF, the same convention is used to generate the residual, however there are extra terms in the residual incorporating stress or minimalization of free energy relative to the lattice parameters of the unit cell θ_i. The additional term in the residual is represented by

$$R = \frac{\partial F}{\partial \theta_i} \tag{2.4.1}$$

with i being the number of independant lattice parameters for the periodic lattice.

The residual generated is minimized using a quasi-Newton Raphson method called the Broyden's method implemented by Qin and Morse.[50] This method reduces the simulation time by generating the Jacobian only once at the start of the iteration algorithm instead of generating a completely new Jacobian for each iteration step in a pure Newton-Raphson implementation. Broyden's method starts with a rough estimate of the Jacobian and improves the estimate of the Jacobian as the number of iterations go up. This speeds up the calulation as one does not have to calulate the Jacobian in each iteration step.

CHAPTER 3

Self Consistent Field Theory study of poly(styrene-*b*-isoprene-*b*-styrene-*b*-ethylene oxide)

This chapter will go over the results obtained using SCFT to study the stability of phases in poly(styrene-*b*-isoprene-*b*-styrene-*b*-ethylene oxide) (SISO) tetrablocks.

Two recent experimental studies have investigated the bulk morphological behavior of poly(styrene-*b*-isoprene-*b*-styrene-*b*-ethylene oxide) (SISO) terpolymers.[1–3] Three isopleths were studied experimentally and the theoretical work mirrors the molecular parameters associated with the experiments.

3.1 Input Parameters

3.1.1 Overview of Experiments

Self-consistent Field Theory(SCFT) calculations were performed along the isopleths studied experimentally by Bluemle et al.[3] and Zhang et al.[2] The isopleths used parent triblock copolymers consisting of poly(styrene-*b*-isoprene-*b*-styrene) (SIS) with $\xi = N_S/N_{S'} = 1$. Experimentally, the tetrablocks were synthesized following a protocol explained in previous work[27,28] to ensure that the only variation in a series of tetrablocks is the length of the O block. The parent triblocks used for these studies contained 50%, 60% and 40% PI.[1] The experimental results obtained for these three isopleths can be found in Table 3.1.

40:60		50:50		60:40	
Mn	23.1 kg/mol	Mn	20.8 kg/mol	Mn	23.3 kg/mol
T	120°C	T	140°C	T	120°C
% EO	Phase	% EO	Phase	% EO	Phase
4	Dis	4	Dis	2	Dis
9	BCC	7	LLP	9	$P6/mmm$
11	LLP	8	LLP	12	$P6/mmm$
15	LLP	9	LLP	19	$P6/mmm$
31	$P6/mm$	12	$P6/mm$	32	$P6/mmm$
35	$P6/mm$	14	$P6/mm$		
		16	$P6/mm$		
		19	$P6/mm$		
		13	$P6/mm$		

Table 3.1: Experimental results for the three isopleths probed with SCFT. These results were determined by Zhang et al.(40:60[1], 60:40[2]) and Bluemle et al.(50:50[3]). The column labels show the parent triblock composition with the notation f_I:f_S and the percent by volume of PEO contained in the tetrablock. The molecular weight of the parent triblock is shown in the second row. The third row contains the temperature at which the experiments were carried out. Phase determination was completed using SAXS and TEM described in detail in the experimental work. 'Dis' marks a disordered phase being viewed. 'BCC' is body centered cubic($Im\bar{3}m$) phase. Liquid like packing(LLP) was indicated by no long range order but local spherical domains viewed via TEM. There are two different hexagonal phases identified in these tetrablocks. $P6/mm$ is hexagonally packed cylinders. $P6/mmm$ is hexagonally packed spheres.

3.1.2 Simulation Stratagies and Parameters

Binary interaction parameters for IS, IO and SO haave been estimated from experimental studies of corresponding diblock copolymers yeilding

$$\begin{aligned} \chi_{IS} &= \tfrac{26.4}{T} - 0.0287 \\ \chi_{IO} &= \tfrac{90.0}{T} - 0.0579 \\ \chi_{SO} &= \tfrac{29.8}{T} - 0.0229 \end{aligned} \tag{3.1.1}$$

These parameters were all determined by fitting the order-disorder transition temperatures of nearly symmetric diblock copolymers.[52,53] These parameters were used in a previous SCFT study of ISO triblock copolymers.[4] An alternate determination of χ_{SO} was made by Frielinghaus. He blended diblock of IS and SO in varying amounts of I. Interaction of SO was determined by fitting the data to the binodal equation. This alternate interaction parameter will be explored later in this chapter. The initial values used for χ determined from Equation 3.1.1 can be found in Table 3.2.

	χ_{SI}	χ_{SO}	χ_{IO}
120°C	0.384499	0.0528980	0.1710206
140°C	0.0351993	0.0492288	0.1599386

Table 3.2: Interaction parameters calculated for the two temperatures used (120°C, 140°C) from the equations shown in Eqn. 3.1.1.

In order to accurately input a χN value in SCFT, a degree of polymerization must be specified . These were determined by using the molecular weight and volume fractions specified in experimental work done by Bluemle et al. and Zhang et al. The reference volume used was 118 $\mathring{A}^3$ and density information is obtained from Fetters.[26] The data given was the molecular weight of the tetrablock as well as the volume fractions of each component. The volume fraction can be expressed as a function of the molecular weight of each block and the corresponding density of the block[26]. Further calculations can be done to obtain the molecular weight of each block and subsequently, the degree of polymerization.

$$N_I = \frac{M_I \frac{1}{\rho_I}}{N_{Av} V_{Ref}} \tag{3.1.2}$$

$$\begin{aligned} N_S &= 14.5\tfrac{mol}{kg} M_S \\ N_I &= 17.0\tfrac{mol}{kg} M_I \\ N_O &= 13.2\tfrac{mol}{kg} M_O \end{aligned} \tag{3.1.3}$$

N_{Av} is Avogadros number and V_{ref} is the reference volume.

The work executed by Bluemle et al. used a parent triblock copolymer with a molecular weight of 20.8 kg/mol. Work completed by Zhang et al. consisted of a parent triblock with a higher molecualar weight (23.1 kg/mol). At a higher molecular weight, Zhang et al. didn't observed the same phases seen by Bluemle et al. so simulations were completed for both parent triblock molecular weights(20.8 kg/mol and 23.1 kg/mol) and subsequent degree of polymerization of the parent triblocks. Table 3.3 shows the parent block number degree of polymerization determined using Eqns 3.1.2-3.1.3, previously determined densities[26] and a reference volume of 118 $\mathring{A}^3$.

	20.8 kg/mol	23.1 kg/mol
60:40	331.0	367.8
50:50	325.0	361.0
40:60	302.0	335.6

Table 3.3: The degree of polymerization of the starting triblock copolymers with f_O=0. The row labels show the parent triblock composition with the notation f_I:f_S.

The simulations were carried out in a way that the only difference between the isopleths studied would be the parent triblock composition. This approach was used to accurately compare the isopleths of higher and lower molecular weight parent triblock terpolymers at the two temperatures used by Bluemle et al. and Zhang et al.

There is a collection of work done studying diblock copolymer morphology in

David Morse's group. The abundance of solutions complete with density profiles for the phases seen led to designing a tetrablock that starts as acting like a diblock and gradually transforming it to a tetrablock. This was done using the polymer profile of a diblock that forms hexagonally packed cylinders with a minority component of 19% by volume. Within the tetrablock, the minority component is the C block. To treat a BABC tetrablock copolymers as a diblock, one must make B and A not interact and have B interact with C the same way A interacts with C. This means χ_{AB}N=0 and χ_{AC}N=χ_{BC}N. The starting point of 19% PEO was used because at this composition, hexagonal packing was observed by both Bluemle et al.[3] and Zhang et al.[2] The dominating interaction parameter in this system is χ_{AC}N so the first step was to obtain a hexagonal structure with χ_{AC}N and χ_{BC}N equal to the final desired value of χ_{AC}N while χ_{AB}=0. This diblock was gradually progressed to the desired tetrablock by increasing χ_{AB}N and decreasing χ_{BC}N. Once the tetrablock with all desired χN values was obtained, further sweeps were done in χN and volume fractions to visualize the entire isopleth looked at by Bluemle et al. and Zhang et al. This process was then again used for the body centered cubic phase starting at 12.5% PEO.

3.2 Diblock Interaction Parameters

3.2.1 Phase Behavior

The free energy difference plot seen in Figure 3.1 shows that the 50:50 isopleth exhibits a very small free energy difference between the hexagonal phase and the $Im\bar{3}m$

phase in the volume fraction where liquid-like packing was seen(f_O=0.07-0.09) experimentally. It should be noted that SCFT can only be used to model spatially periodic structures, and cannot explicitliy describe the liquid like packing observed via TEM. In regions where a liquid-like arrangement of spheres is seen experimentally, it can be expected that the BCC arrangement of spheres to have a lower free energy than the cylinder phase. Here, the BCC phase is a surrogate for any sphere packing. The small difference in free energy can be seen more easily in a close up of the free energy difference with small volume fractions of PEO. This can be seen in Figure 3.2. For this up close view it is evident that the BCC phase has a small window of volume fraction where it is the preferred phase instead of cylinders and the disordered state.

Small difference in free energy is a sign that this system is near a critical point. The small energy difference can be seen in diblock copolymers near the critical point that occurs when χN=10.495. The free energy difference between the BCC phase, the hexagonal phase and the disordered phase is very small. The small energy difference seen in Figure 3.2 suggests that at this small amount of PEO may be near the critical point. Investigatation into the critical point lead to probing the lamellar phase being the phase with the lowest free energy phase for this tetrablock. The parent SIS triblock of all systems studied is disordered. The dominating interaction parameter that causes phase separation for this system is between the PI domain and the PEO domain. The lamellar phase would contain layers of the PS with small amounts of PEO and PI domains. At lower PEO volume fractions, the lowest free energy phase is disordered because the interaction parameter is not large enough to force domains to separate. Many different paths were completed in an attempt to find a place where

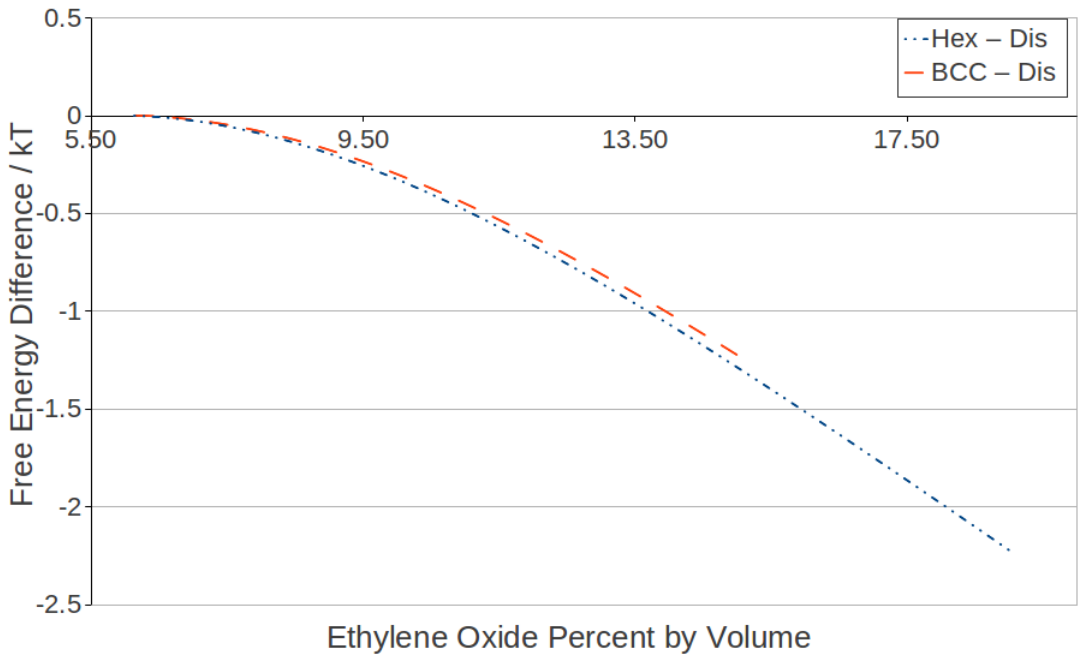

Figure 3.1: Expanded view of free energy difference for the 50:50 (f_I:f_S) parent triblock copolymer between hexagonally packed cylinders(Hex) and disordered divided by kT as well as the difference between the body centered cubic spheres(BCC) and disordered divided by kT vs. percent PEO by volume. A closer view of the free energy difference at low amounts of PEO can be seen in Figure 3.2

this phase was stable. The multiple steps taken did not result in a stable lamellar phase being seen.

To know where the cross over from BCC to hexagonal packing takes place, a free energy difference between the disordered state and the two states of interest was calculated. It can be see in Figure 3.2. This plot shows that the place where the BCC phase becomes the most stable is near 6.38% volume PEO. This agrees with the phases viewed by Bluemle et al. at these volume fractions. Liquid like packing was seen at this volume fraction. The determination of liquid like packing

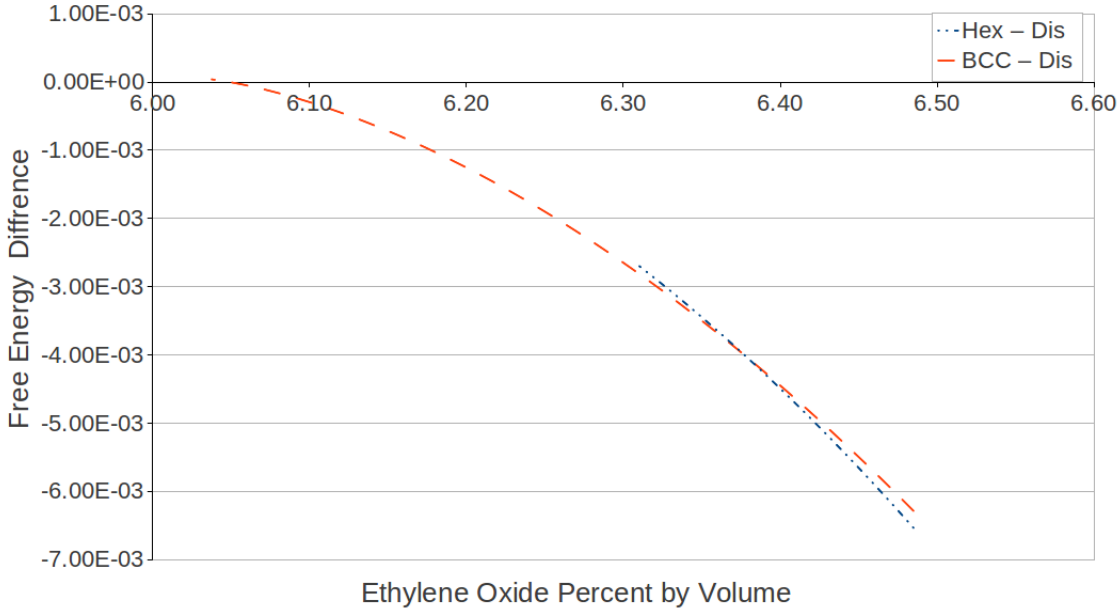

Figure 3.2: Free energy difference for the 50:50 (f_I:f_S) parent triblock copolymer between hexagonally packed cylinders(Hex) and disordered divided by kT as well as the difference between the body centered cubic spheres(BCC) and disordered divided by kT vs. percent PEO by volume. This plot was done at low PEO volume fractions to better see where phase transitions take place. It can be seen that at near 6.38% volume PEO, the BCC structure has a lower free energy than the hexagonal structure. At approximately 6.05% volume PEO, the disordered state has the lowest free energy. This was completed for a triblock with a molecular weight of 20.8 kg/mol at 140 °C and corresponds to the isopleth looked at by Bluemle et al.[3]

was based on the sighting of spheres with no long range order. The theory predicts that there is long range order more stable than the partially disordered phase viewed via transmission electron microscopy. The disordered phase is the most stable for volume fractions lower than 6.05%. The location of the disordered phase is consistent with experimental results. Differences in free energy were calculated along all isopleths at two temperatures. These results can be seen in Table 3.4.

		High Mn (23.1 kg/mol)			Low Mn (20.8 kg/mol)		
		40:60	50:50	60:40	40:60	50:50	60:40
140 °C	Dis - BCC	6.725	4.775	4.725	8.100	6.0475	5.7525
	BCC - Hex	6.750	4.900	5.725	8.350	6.3775	7.3175
120 °C	Dis - BCC	5.725	4.400	3.975	7.100	5.110	5.005
	BCC - Hex	5.800	4.450	4.625	7.175	5.260	6.100

Table 3.4: Phase transitions from Disordered to BCC as well as from BCC to hexagonal cylinders. These were determined by comparing the free energies of the phases. The column labels show the parent triblock composition with the notation f_I:f_S.

3.2.2 Unit Cell Parameters

The set of simulations produce a lattice dimension that can be translated into domain spacing. Table 3.5 contains the experimentally determined domain compared to the theroetically determined domain space. The theoretical data was chosen so that it would match the experimental parameters. There is very close agreement between the theory and the experiment results for high amounts of PEO (14 - 19% PEO) where theory showed the hexagonal phase as having the lowest free energy. In the regime where liquid-like packing was seen experimentally, theory predicted that the hexagonal phase had the lowest free energy. There is a far greater amount of symmetry in the BCC phase, as most likely the liquid-like packing phase compared to the cylinderical phase. This major differences in structure symmetry of these states can explain the vast difference between the experimental results and the theory prediction.

3.2.3 Composition Profiles

The isopleths investigated by Bluemle et al. and Zhang et al. were studied in this work. To ensure capture of hexagonally packed cylinders, visualization of the $P6/mm$

Percent poly(Ethylene Oxide)	Experimental Lattice Size	Theory Lattice Size
7	17.6 nm	14.75 nm
9	18.9 nm	16.10 nm
14	20.0 nm	18.76 nm
16	20.9 nm	19.81 nm
19	22.2 nm	21.31 nm

Table 3.5: Comparison of experimentally determined lattice size by Bluemle et al.[3] and as predicted by theory for the $P6/mm$ phase. The simulations were done at 140 °C with a 50:50 parent triblock and a molecular weight of 20.8 kg/mol to match experimental conditions. The notation for parent triblock compostion is f_I:f_S.

phase was completed. The polymer profile visualization of the $P6/mm$ phase for the PEO volume of 19% seen by Bluemle et al. can be seen in Figure 3.3. The profile shows hexagonally packed cylinders of PEO surrounded by PS in a matrix of mixed PS and PI. The largest and dominating interaction parameter is between PEO and PI so it is expected to observe these not mixing. The interaction between PI and PS is not strong. Both of these phenomenon explain why it appears the cylinders of PEO are surrounded by PS located in a matrix containing both PS and PI. This visualization was also done for the isopleth containing the 60% volume PI parent triblock. In general, there was no difference in the polymer profile except for the matrix surrounding the cylinders consisted a larger amount of PI.

Polymer segregation in these ordered phases is also of interest. To investigate the local structure, a density profile was obtained. The plot in Figure 3.4 is the amount a polymer at a point along the unit cell. This was done along the [100] direction for hexagonally packed cylinders. The profile is from the center of one cylinder to the center of the its nearest neighbor and shows the locations of concentrated type of

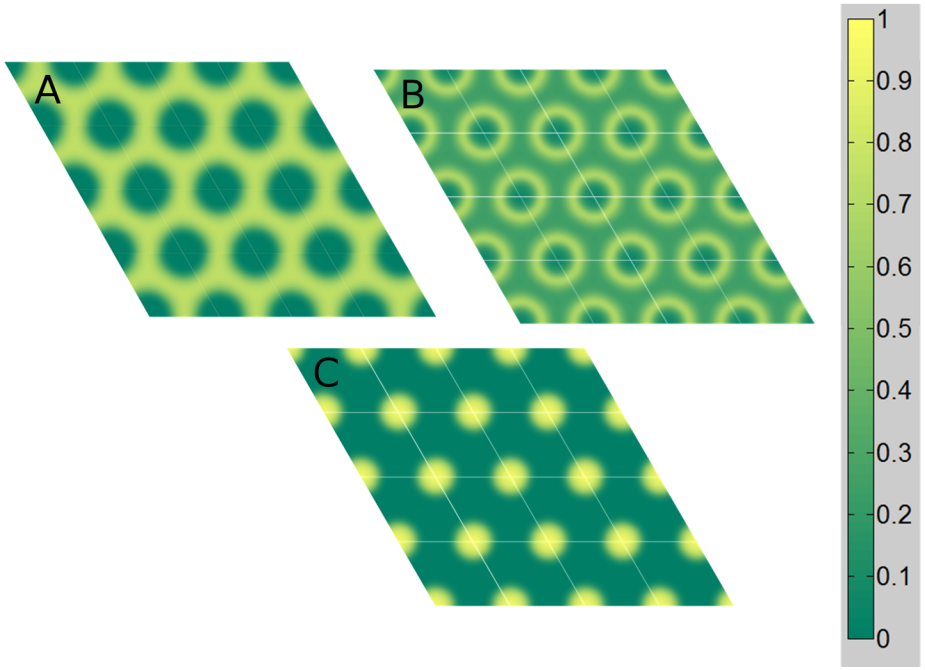

Figure 3.3: Polymer density profiles of PI(A), PS(B), and ethlylene oxide(C) in the $P6/mm$ phase. This phase was reported in experimental work completed by Bluemle et. al.[3] Images correspond to the simulations done by SCFT with the following volume fractions: f_S=0.40, f_I=0.41 and f_O=0.19 at 140 °C with a parent triblock molecular weiht of 20.8 kg/mol. All interaction parameters can be found in Table 3.2.

polymer. This diagram shows that the cylinders are mostly PEO surrounded by PS in a matrix that is a mixture of PS and PI.

The density profile yields valuable information about the segregation that occurs in the unit cell. Here is it also seen that since the largest interaction parameter is between PEO and PI, they are seen to be strongly segregated. The interaction between PI and PS is not strong, therefore; the cylinders of PEO are surrounded by PS located in a matrix containing both PS and PI. These results confirm the separation seen by the polymers in Figure 3.3.

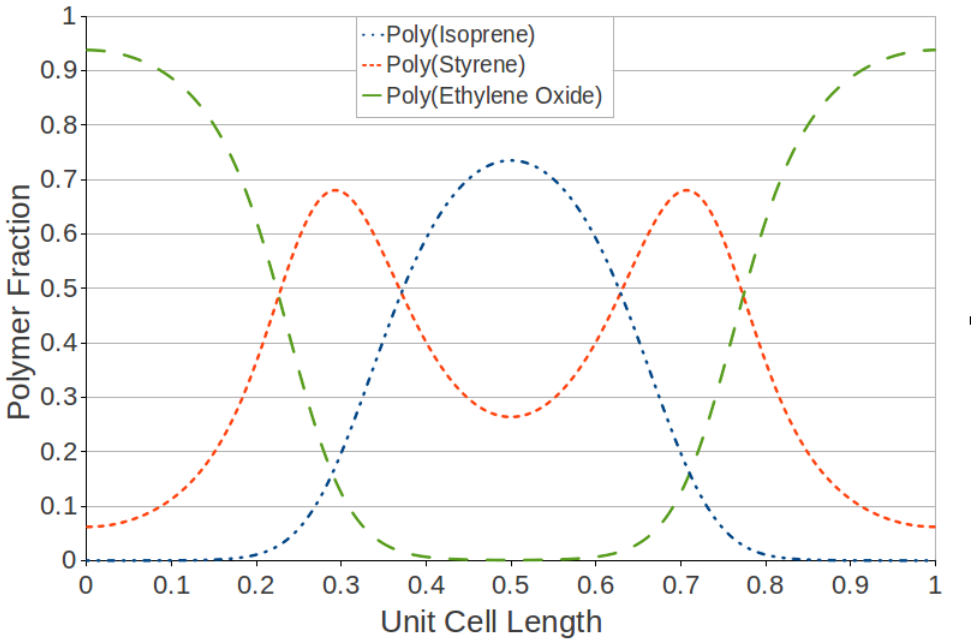

Figure 3.4: Plot of polymer density profiles for the $P6/mm$ phase along the [100] unit cell direction determined by SCFT for the following volume fractions: f_S=0.40, f_I=0.41 and f_O=0.19 at 140 °C.

The small difference in free energy between the $P6/mm$ phase, BCC phase and a disordered mixture at low PEO volume fractions led us to probe the segregatation at lower PEO content. The density profile for the $P6mm$ phase that occurs with a small amount of PEO (6.38% by volume) can be seen in Figure 3.5. With slightly less PEO (6.3775% by volume) the BCC phase becomes the state with the lowest free energy.

It was also of interest to look at the segregation of the polymers in the BCC phase. A look along the [111] unit cell direction is the best way to do this. The $Im\bar{3}m$ polymer density can be seen in Figure 3.6. This is the profile with 6.36% volume PEO. This state is also close in free energy to the disordered phase. There is not a

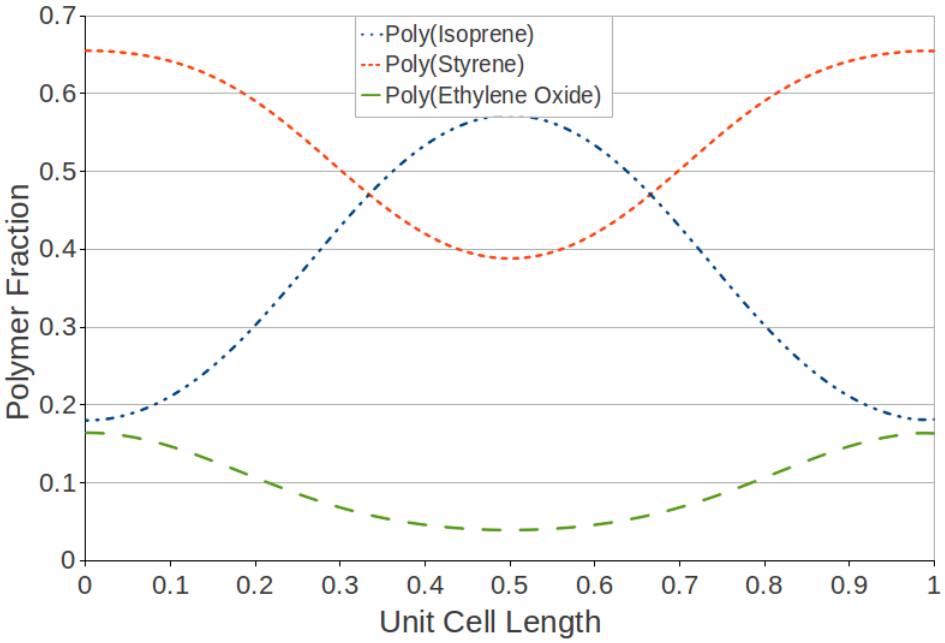

Figure 3.5: Polymer density profiles for the $P6/mm$ phase along the [100] unit cell direction determined by SCFT for the following volume fractions: f_S=0.4775, f_I=0.4587 and f_O=0.0638 at 140 °C.

lot of segregation between blocks in this phase with the given interaction parameters. This does not appear as if it would show any difference in electron density that one would see in TEM. This contradicts the visualization of spheres with no long range of order seen by Bluemle et al. with $f_O = 0.07 - 0.09$.[3]

Experiment and theory both predict hexagonally packed cylinders to be stable at large amounts of PEO (10- 19%) among the three isopleths studied. The composition profiles clearly show cylinders of PEO surrounded by PS in a matrix of PS and PI. The only difference for any of the isopleths was the PS-PI matrix that contained the cylinders of PEO. The predicted domain spacing does not deviate largely from the experimental spacing obtained via SAXS in this region. There are some substantial

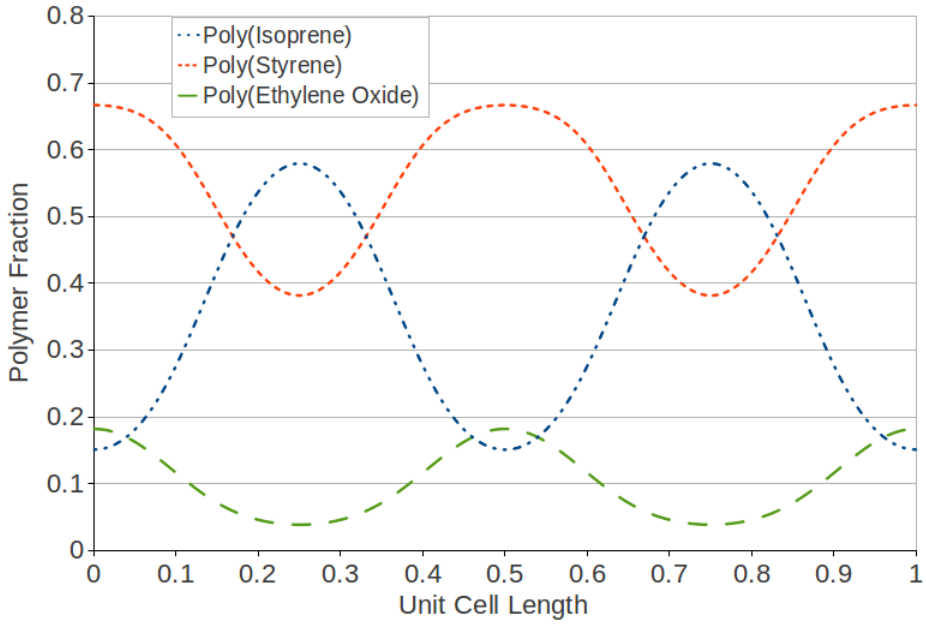

Figure 3.6: Polymer density profiles determined for the $Im\bar{3}m$ phase along the [111] unit cell direction by SCFT for the following volume fractions: f_S=0.46746, f_I=0.46904 and f_O=0.0636 at 140 °C.

differences with lower amounts of PEO (less than 10%). For the 40:60 and 50:50 isopleths (f_I:f_S), experimental work determined liquid-like packing at low amounts of PEO. Thoery predicts only a small window where sphere packing has the lowest free energy. For the 60:40 isopleth, theory determines hexagonally packed cylinders to be stable but no work was done to determine if the sphere phase has a lower free energy. Along all three isopleths, there is general good agreement on where the disordered phase becomes the most stable. Attempts will be made to match theory with experiment more closely in low amounts of PEO (less than 10%). The easiest parameter to modify is the interaction parameters of all species. The next two sections with explore the adjustments made to interaction parameters.

3.3 Increase and Decrease χ_{IO} and χ_{SO}

Previous work done on ISO triblock copolyers used the interaction parameters come from the paper published by Frielinghaus.[4] These parameters were determined with a variety of experiments done with diblock copolymers. It is noted in a second publication that the formulas for χ are subject to a considerable error, $\pm$ 10%.[53] This acknowledgement led to a probe of altering the interaction parameters. The interaction of PS and PI has been highly studied and reported; therefore, it was not probed in this study. An increase and decrease in χ_{IO} and χ_{SO} was done at 140 °C along the same volume fractions probed earlier. The interaction parameters used for this set of simulations can be found in Table 3.6

	χ_{IO}	χ_{SO}
10% Increase	0.175932	0.054152
20% Increase	0.211119	0.059074
10% Decrease	0.145397	0.044753
20% Decrease	0.121166	0.037294

Table 3.6: Interaction parameter values used when probing the effects of increasing and decreasing χ. These are the increases and decreases calculated based on the values obtained by using Equation 3.1.1 at 140°.

Table 3.7 contains the data attained with changes in the interaction parameters. There is not a large change in the length of the region where BCC is stable, merely a general increase or decrease in the area that the small window takes place. An increase in the interaction between PS and PEO shows an increase in the amount of PEO needed for the BCC phase to be lower in free energy compared to the disordered phase. It is expected that increasing the interaction means less polymer is needed to make a phase stable. The opposite happens here because the frustration of the

system is increased when the interaction parameter is increased. This phenomenon has been seen in previous work.[27]

		χ_{IO}	% Change	χ_{SO}	% Change
10% Increase	Dis - BCC	5.350	-11.534	6.175	2.108
	BCC - Hex	5.625	-11.799	6.600	3.489
20% Increase	Dis - BCC	4.225	-30.136	6.325	4.589
	BCC - Hex	4.425	-30.615	6.875	7.801
10% Decrease	Dis - BCC	6.900	8.193	5.875	-2.852
	BCC - Hex	7.275	14.073	6.150	-3.567
20% Decrease	Dis - BCC	8.850	46.341	5.625	-6.986
	BCC - Hex	9.600	50.529	5.850	-8.271

Table 3.7: Phase transitions from Disordered to BCC as well as from BCC to hexangonal cylinders. These were determined by comparing the free energy of the phases. These simulations were completed using a 50:50 parent triblock and changing the interaction parameters as determined by diblock copolymers at 140 °C. The % change is calculated in relatation to the phase transitions calculated using the pure diblock interaction parameters found in Table 3.4.

3.4 Alternate χ_{SO}

There has been work done to show that the actual χ parameter can be up to twice as much as predicted by theory.[54] A set of simulations was done with double the χ parameters obtained in Equation 3.1.1. The values of χ used can be found in Table 3.8

χ_{SI}	χ_{IO}	χ_{SO}
0.076899	0.342045	0.105796

Table 3.8: Interaction parameters used when probing the effects of doubling χ determined from diblock copolymer results at 140°.

This doubling destabilized the region where any BCC phase was stable. The

double interaction parameter between PS and PI led the the parent triblock having order, which not seen in any experimental work.[1–3] Previous theoretical work on this tetrablock did not find a location where lamellae was the lowest free energy structure so it was not studied under this change in interaction. The run of simulations with double interaction shows that not every interaction parameter is off by a factor of 2. The PI-PS interaction has been studied in great detail and is well understood. The other interactions are not as well studied so there may be some discrepancy between the reported equations and the actual equations.

There was an additional equation for χ_{SO} given in the work done by Frielinghaus.[53] The alternate equation for χ_{SO} can be found in Equation 3.4.1. This interaction parameter was determined by mixing homopolymers of PS and PEO. There is a large difference in both the enthalpic and entropic terms of the equation. A new value of χ_{SO} was calculated. All interaction parameters used in this set of simulations can be found in Table 3.9.

$$\chi_{SO} = \frac{72.9}{T} - 0.0810 \tag{3.4.1}$$

	χ_{SI}	χ_{SO}	χ_{IO}
120°C	0.384499	0.1044254	0.1710206

Table 3.9: Alternate χ_{SO} interaction parameter calculated using Eqn 3.4.1. Interaction parameters χ_{SI} and χ_{IO} were calculated using Eqn 3.1.1. All calculations were done using a temperature of 120°C.

		High Mn (23.1 k/mol)			Low Mn (20.8 k/mol)		
		40:60	50:50	60:40	40:60	50:50	60:40
120 °C	Dis - BCC	8.250	7.475	6.500	9.175	8.000	7.375
	BCC - Hex	11.250	10.425	10.150	12.200	11.000	11.025

Table 3.10: Phase transitions from Disordered to BCC as well as from BCC to hexagonal cylinders. These were determined by comparing the free energy of the phases. The phase with the lowest free energy is the most stable. The column labels show the parent triblock composition with the notation f_I:f_S. These simulations were completed using the diblock determined interaction parameters for χ_{SI} and χ_{IO} and the interaction parameter determined by blending homopolymers for χ_{SO}. This group of simulations was completed at 120 °C.

3.4.1 Phase Behavior

The isopleths investigated with the earlier equation for χ_{SO} were probed with this new equation. The results can be seen in Table 3.10. The window where BCC is the most stable phase greatly increases from less than 0.5% to 3%. More PEO is needed for BCC to be stable over the disordered phase. This is also due to increasing the frustration of the system.[27] Separating the PS and PEO requires more free energy when a higher interaction parameter is used.

3.4.2 Unit Cell Parameters

Again, the set of simulations produce a lattice dimension that can be translated into domain spacing. Table 3.11 contains the experimentally determined domain compared to the theroetically determined domain space. The theoretical data was chosen so that it would match the experimental composition parameters. There is very close agreement between the theory and the experiment results for high amounts of PRO (14 - 19% PEO) where theory showed the hexagonal phase as having the lowest free

energy. Liquid-like packing was seen at 9% PEO where theory showed hexagonally packed cylinders had the lowest free energy. Again, the vast differences in the amount of symmetry in the phases viewed could account for the large difference between theory and experimentally determined lattice dimensions.

Percent poly(Ethylene Oxide)	Experimental Lattice Size	Theory Lattice Size
9	18.9 nm	16.75 nm
14	20.0 nm	20.06 nm
16	20.9 nm	21.23 nm
19	22.2 nm	22.90 nm

Table 3.11: Comparison of experimentally determined lattice size by Bluemle et al.[3] and as predicted by theory using the χ values seen in Table 3.9. The simulations were done with a 50:50 parent triblock and a molcular weight of 20.8 kg/mol to match experimental conditions. The notation for parent triblock compostion is f_I:f_S.

3.4.3 Composition Profiles

Once again, segregation between polymer blocks was of interest to try to understand the observation of liquid-like packing observed in previous work.[3] The density profile along the [111] unit cell direction for the BCC phase can be seen in Figure 3.7. Figure 3.7 shows a strong segregation of domains which leads to very different electron densities appearing as spheres in TEM images. These results imply that the interaction parameters are a complex problem that is not fully understood. Theory results do confirm that there is a region where spheres are the most stable phase for these tetrablock terpolymers but the location of this region differs from the experimentally observed region.

Thoery predictions match more closely to the experimental results that have been seen. The distinct layers seen in the BCC density profile would be seen in a TEM due to differences in electron densities in the layers. Experimentally determined domain spacing closely matches thoery with this alternate interaction parameter. These can be seen in Table 3.5. Although the domain spacing in slightly higher for the theory than is seen experimentally, they are close in value.

The increase in χ_{SO} does not change experiment and theory predicting hexagonally packed cylinders to be stable at large amounts of PEO (10- 19%) among the three isopleths studied. Once again, the composition profiles clearly show cylinders of PEO surrounded by PS in a matrix of PS and PI. The predicted domain spacing does not deviate largely from the experimental spacing obtained via SAXS in this region. An increase in χ_{SO} changes the window where sphere packing is seen as well as the width of this region. Along the 40:60 isopleth (f_I:f_S), there is agreement in where the BCC

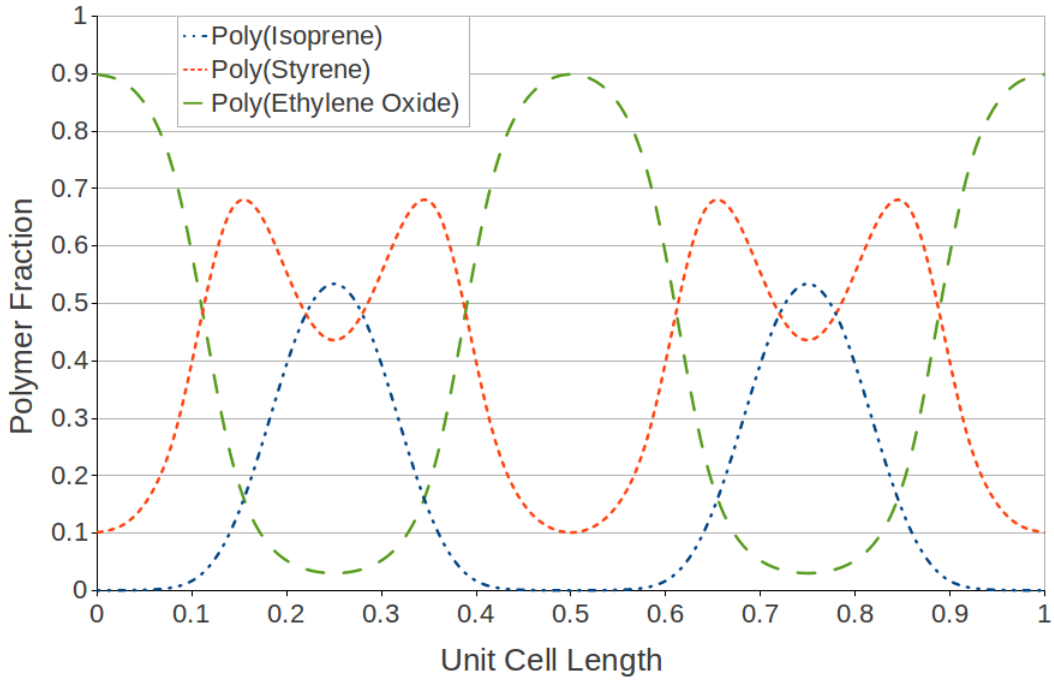

Figure 3.7: Polymer desnity profiles determined for the $Im\bar{3}m$ phase along the [111] unit cell direction by SCFT for the following volume fractions: f_S=0.44333, f_I=0.44792 and f_O=0.10875 at 120 °C.

phase is the mose stable. There was liquid-like packing viewed at higher amount of PEO (11-15%) where theory showed hexagonally packed cylinders had the lowest free energy. The 50:50 isopleth showed much better agreement between experiment and theory. Experiments showed liquid-like packing from 7-9% PEO. The region where BCC had the lowest free energy is between 8-11% PEO. The 60:40 isopleth, theory determines hexagonally packed cylinders to the stable but no work was done to determine if the sphere phase has a lower free energy. Along all three isopleths, there is general good agreement on where the disordered phase becomes the most stable.

3.5 Conclusions

This thesis focused on examining the phase formation of tetrablock terpolymers using self-consistent field theory. The polymer investigated is poly(styrene-*b*-isoprene-*b*-styrene-*b*-ethylene oxide). The experimental work done on these polymers was acheived by anionic polymerization and subsequent characterization via GPC, NMR, TEM and scattering data.

SCFT was used to study this system with different compostion parent triblocks for the series of tetrablocks. The system of SISO is of experimental interest because a parent triblock can be used to make a series of tetrablocks.[27,28] The use of the same parent triblock means the isopleth can be exactly studied.

There has been no attempt to simulate the σ-phase because of it's complexity. The experimentally viewed $P6/mmm$ phase of hexagonally packed spheres was also not explored. There is a possibility that one of these phases is lower in free energy than the tested $P6/mm$ and $Im\overline{3}m$ phases.

SCFT simulations that have allowed for disorder, BCC, hexagonally packed cylinders and lamellar phase yield a phase sequence disordered-BCC-Hex with increasing amounts of ethlyene oxide in SISO tetrablocks along the three isopleths studied here. This is in general qualitative agreement with experimental work in which the parent triblocks have f_I:f_S = 40:60 and 50:50 if the BCC phase is associated with liquid-like packing.

When using the diblock determined interaction parameters, the BCC phase is stable only over a narrow range of compositions, much narrower than the range where liquid-like packing was seen with the f_I:f_S=40:60 and 50:50 parent triblock copoly-

mers. For the 50:50 system studied by Bluemle et al. (20.8 kg/mol, 140°C), the BCC phase is found to be stable over a 0.3% window whereas the liquid-like packing was seen over at least 2%. For the 40:60 system studied by Zhang (23.1 kg/mol, 120°C), the BCC phase is found to be stable over a 0.1% window whereas the liquid-like packing was seen over at least 4%. The use of the χ_{SO} determined by blending of polymers changed the window where BCC was seen to 3% for both isopleths.

For the f_I:f_S = 60:40 isopleth Zhang et al. claimed to find a large region where a $P6/mmm$ phase is stable. SCFT predicts a free energy for the $P6/mm$ phase of the hexagonal cylinders lower than for the BCC sphere phase throughout the range of values of f_O in which Zhang et al. reported a simple hexagonal 3D crystal of spheres. For the system studied by Zhang et al. (23.1 kg/mol 120°C), SCFT predicts hexagonally packed cylinders for all $f_O > 4.7\%$ whereas Zhang et al. reported hexagonall packed spheres for f_O = 9 - 32%, but did not report a structure for smaller values of f_O. It is hard to trust the spherical morphology was seen at such high PEO based on the trend predicted by SCFT as well as the phases viewed in other experiments where increasing f_O leads to a tranformation to a cylinderical morphology at much lower f_O.

Bibliography

[1] Zhang, J., 2012. Phase behaviors of ABAC tetrablock terpolymers. Ph.D. thesis, University of Minnesota.

[2] Zhang, J., S. Scott, and B. Frank S., 2012. Ordering of sphere formingsiso tetrablock terpolymers on a simple hexagonal lattice. *Macromolecules* 45:256 – 265.

[3] Bluemle, M. J., J. Zhang, T. P. Lodge, and F. S. Bates, 2010. Inverted phases induced by chain architecture in abac tetrablock terpolymers. *Macromolecules* 43:4449 – 4452.

[4] Tyler, C. A., and D. C. Morse, 2005. Orthorhombic $fddd$ network in triblock and diblock copolymer melts. *Phys. Rev. Lett.* 94:208302.

[5] Bluemle, M. J., G. Fleury, T. P. Lodge, and F. S. Bates, 2009. The o52 network by molecular design: Cecd tetrablock terpolymers. *Soft Matter* 5:1587–1590.

[6] Lee, S., M. J. Bluemle, and F. S. Bates, 2010. Discovery of a frank-kasper phase in sphere-forming block copolymer melts. *Science* 330:349 – 353.

[7] Lodge, T. P., 2003. Block copolymers: Past successes and future challenges. *Macromolecular Chemistry and Physics* 204:265–273.

[8] Matsen, M. W., and F. S. Bates, 1997. Conformationally asymmetric block copolymers. *Journal of Polymer Science Part B: Polymer Physics* 35:945–952.

[9] Matsen, M. W., 2007. Polydispersity-induced macrophase separation in diblock copolymer melts. *Phys. Rev. Lett.* 99:148304.

[10] Hajduk, D. A., P. E. Harper, S. M. Gruner, C. C. Honeker, G. Kim, E. L. Thomas, and L. J. Fetters, 1994. The gyroid: A new equilibrium morphology in weakly segregated diblock copolymers. *Macromolecules* 27:4063–4075.

[11] Schulz, M. F., A. K. Khandpur, F. S. Bates, K. Almdal, K. Mortensen, D. A. Hajduk, and S. M. Gruner, 1996. Phase behavior of polystyrenepoly(2-vinylpyridine) diblock copolymers. *Macromolecules* 29:2857–2867.

[12] Takenaka, M., T. Wakada, S. Akasaka, S. Nishitsuji, K. Saijo, H. Shimizu, M. I. Kim, and H. Hasegawa, 2007. Orthorhombic fddd network in diblock copolymer melts. *Macromolecules* 40:4399–4402.

[13] Epps, T. H., E. W. Cochran, C. M. Hardy, T. S. Bailey, R. S. Waletzko, and F. S. Bates, 2004. Network phases in abc triblock copolymers. *Macromolecules* 37:7085–7088.

[14] Chatterjee, J., S. Jain, and F. S. Bates, 2007. Comprehensive phase behavior of poly(isoprene-b-styrene-b-ethylene oxide) triblock copolymers. *Macromolecules* 40:2882–2896.

[15] Epps, T. H., E. W. Cochran, T. S. Bailey, R. S. Waletzko, C. M. Hardy, and F. S. Bates, 2004. Ordered network phases in linear poly(isoprene-b-styrene-b-ethylene oxide) triblock copolymers. *Macromolecules* 37:8325–8341.

[16] Mogi, Y., H. Kotsuji, Y. Kaneko, K. Mori, Y. Matsushita, and I. Noda, 1992. Preparation and morphology of triblock copolymers of the abc type. *Macromolecules* 25:5408–5411.

[17] Stadler, R., C. Auschra, J. Beckmann, U. Krappe, I. Voight-Martin, and L. Leibler, 1995. Morphology and thermodynamics of symmetric poly(a-block-b-block-c) triblock copolymers. *Macromolecules* 28:3080–3097.

[18] Breiner, U., U. Krappe, V. Abetz, and R. Stadler, 1997. Cylindrical morphologies in asymmetric abc triblock copolymers. *Macromolecular Chemistry and Physics* 198:1051–1083.

[19] Shefelbine, T. A., M. E. Vigild, M. W. Matsen, D. A. Hajduk, M. A. Hillmyer, E. L. Cussler, and F. S. Bates, 1999. Coreshell gyroid morphology in a poly(isoprene-block-styrene-block-dimethylsiloxane) triblock copolymer. *Journal of the American Chemical Society* 121:8457–8465.

[20] Zheng, W., and Z.-G. Wang, 1995. Morphology of abc triblock copolymers. *Macromolecules* 28:7215–7223.

[21] Jiafang, W., M. Mller, and W. Zhen-Gang, 2009. Nucleation in a/b/ab blends: Interplay between microphase assembly and macrophase separation. *Journal of Chemical Physics* 130:154902.

[22] Tyler, C. A., J. Qin, F. S. Bates, and D. C. Morse, 2007. Scft study of nonfrustrated abc triblock copolymer melts. *Macromolecules* 40:4654–4668.

[23] Qin, J., F. S. Bates, and D. C. Morse, 2010. Phase behavior of nonfrustrated abc triblock copolymers: Weak and intermediate segregation. *Macromolecules* 43:5128–5136.

[24] Cochran, E. W., and F. S. Bates, 2004. Shear-induced network-to-network transition in a block copolymer melt. *Phys. Rev. Lett.* 93:087802.

[25] Bates, F. S., M. A. Hillmyer, T. P. Lodge, C. M. Bates, K. T. Delaney, and G. H. Fredrickson, 2012. Multiblock polymers: Panacea or pandoras box? *Science* 336:434–440.

[26] Fetters, L. J., D. J. Lohse, D. Richter, T. A. Witten, and A. Zirkel, 1994. Connection between polymer molecular weight, density, chain dimensions, and melt viscoelastic properties. *Macromolecules* 27:4639–4647.

[27] Bailey, T. S., H. D. Pham, and F. S. Bates, 2001. Morphological behavior bridging the symmetric ab and abc states in the poly(styrene-b-isoprene-b-ethylene oxide) triblock copolymer system. *Macromolecules* 34:6994–7008.

[28] Hillmyer, M. A., and F. S. Bates, 1996. Synthesis and characterization of model polyalkanepoly(ethylene oxide) block copolymers. *Macromolecules* 29:6994–7002.

[29] Hardy, C. M., F. S. Bates, M.-H. Kim, and G. D. Wignall, 2002. Model abc triblock copolymers and blends near the orderdisorder transition. *Macromolecules* 35:3189–3197.

[30] Goldacker, T., and V. Abetz, 1999. Coreshell cylinders and coreshell gyroid morphologies via blending of lamellar abc triblock and bc diblock copolymers. *Macromolecules* 32:5165–5167.

[31] Fornasini, M. L., P. Manfrinetti, and D. Mazzone, 2006. Ybznal ternary system: Cacu5-type derived compounds in the zinc-rich corner. *Journal of Solid State Chemistry* 179:2012 – 2019.

BIBLIOGRAPHY

[32] Bates, F. S., R. E. C ohen, and C. V. Berney, 1982. Small-angle neutron scattering determination of macrolattice structure in a polystyrene-polybutadiene diblock copolymer. *Macromolecules* 15:589–592.

[33] Leibler, L., 1980. Theory of microphase separation in block copolymers. *Macromolecules* 13:1602–1617.

[34] Xiangbing Zeng, A. J., G. Ungar, G. Yongson Liu, V. Percec, A. E. Dulcey, and J. K. Hobbs, 2004. Supramolecular dendritic liquid quasicrystals. *Nature* 428:157 – 160.

[35] Ungar, G., Y. Liu, X. Zeng, V. Percec, and W.-D. Cho, 2003. Giant supramolecular liquid crystal lattice. *Science* 299:1208.

[36] Zhang, J., and F. S. Bates, 2012. Dodecagonal quasicrystalline morphology in a poly(styrene-b-isoprene-b-styrene-b-ethylene oxide) tetrablock terpolymer. *Journal of the American Chemical Society* 134:7636 – 7639.

[37] Ungar, G., and X. Zeng, 2005. Frank-kasper, quasicrystalline and related phases in liquid crystals. *Soft Matter* 1:95–106.

[38] Matsen, M. W., and F. S. Bates, 1996. Origins of complex self-assembly in block copolymers. *Macromolecules* 29:7641–7644.

[39] Edwards, S. F., 1965. The statistical mechanics of polymers with excluded volume. *Proceedings of the Physical Society* 85:613.

[40] Helfand, E., and Y. Tagami, 1971. Theory of the interface between immiscible polymers. *Journal of Polymer Science Part B: Polymer Letters* 9:741–746.

[41] Helfand, E., and A. M. Sapse, 1975. Theory of unsymmetric polymer–polymer interfaces. *The Journal of Chemical Physics* 62:1327–1331.

[42] Helfand, E., 1975. Block copolymer theory. iii. statistical mechanics of the microdomain structure. *Macromolecules* 8:552–556.

[43] Helfand, E., 1975. Theory of inhomogeneous polymers: Fundamentals of the gaussian random-walk model. *The Journal of Chemical Physics* 62:999–1005.

[44] Helfand, E., and Z. R. Wasserman, 1977. Statistical thermodynamics of microdomain structures in block copolymer systems. *Polymer Engineering & Science* 17:582–586.

BIBLIOGRAPHY

[45] Helfand, E., and Z. R. Wasserman, 1976. Block copolymer theory. 4. narrow interphase approximation. *Macromolecules* 9:879–888.

[46] Helfand, E., 1975. Block copolymers, polymer-polymer interfaces, and the theory of inhomogeneous polymers. *Accounts of Chemical Research* 8:295–299.

[47] Helfand, E., and Z. Wasserman, 1982. Microdomain structure and the interface in block copolymers.(retroactive coverage). *Applied Science Publishers Ltd., Developments in Block Copolymers.* 1:99–125.

[48] Matsen, M. W., and M. Schick, 1994. Stable and unstable phases of a diblock copolymer melt. *Phys. Rev. Lett.* 72:2660–2663.

[49] Rasmussen, K., and G. Kalosakas, 2002. Improved numerical algorithm for exploring block copolymer mesophases. *Journal of Polymer Science Part B: Polymer Physics* 40:1777–1783.

[50] Qin, J., 2009. Studies of Block Copolymer Melts by Field Theory and Molecular Simulation. Ph.D. thesis, University of Minnesota.

[51] Tyler, C., 2005. Linear elasticity and phase behavior of block copolymer melts by self consistent field theory. Ph.D. thesis, University of Minnesota.

[52] Frielinghaus, H., N. Hermsdorf, R. Sigel, K. Almdal, K. Mortensen, I. W. Hamley, L. Mess, L. Corvazier, A. J. Ryan, D. van Dusschoten, M. Wilhelm, G. Floudas, and G. Fytas, 2001. Blends of ab/bc diblock copolymers with a large interaction parameter . *Macromolecules* 34:4907–4916.

[53] Frielinghaus, H., N. Hermsdorf, K. Almdal, K. Mortensen, L. Mess, L. Corvazier, J. P. A. Fairclough, A. J. Ryan, P. D. Olmsted, and I. W. Hamley, 2001. Micro- vs. macro-phase separation in binary blends of poly(styrene)-poly(isoprene) and poly(isoprene)-poly(ethylene oxide) diblock copolymers. *EPL (Europhysics Letters)* 53:680.

[54] Khandpur, A. K., S. Foerster, F. S. Bates, I. W. Hamley, A. J. Ryan, W. Bras, K. Almdal, and K. Mortensen, 1995. Polyisoprene-polystyrene diblock copolymer phase diagram near the order-disorder transition. *Macromolecules* 28:8796–8806.